Chemistry Research Journal, 2022, 7(1):55-68

Available online www.chemrj.org

Research Article

ISSN: 2455-8990
CODEN(USA): CRJHA5

A Density Functional Theory inquiry of the relationships between electronic structure and anticonvulsant activity in a series of 2,5-disubstituted thiadiazoles

Juan S. Gómez-Jeria[1,2*], Carlos Soloaga-Ardiles[3]

[1]Quantum Pharmacology Unit, Department of Chemistry, Faculty of Sciences, University of Chile. Las Palmeras 3425, Santiago 7800003, Chile
[2]Glowing Neurons Group, CP 8270745 Santiago, Chile
[3]Departamento de Química, Facultad de Ciencias, Universidad de Tarapacá. Avenida General Velásquez 1775, Casilla 7D, Arica-Chile
* facien03@uchile.cl

Abstract The Klopman-Peradejordi-Gómez formal QSAR equation was employed for searching quantitative relationships between the electronic structure of a group of 2,5-disubstituted thiadiazoles and their *in vivo* anticonvulsant activity. The study was carried out within the Density Functional Theory at the B3lYP/6-31G(d,p) level with full geometry optimization. A statistically significant equation was obtained (n=14, adj-R^2=0.93, F(4,9)=42.445 (p<0.00001), SD=0.06). The analysis of the equation allowed us to propose some interactions that should be useful in the design of new molecules with better *in vivo* anticonvulsant activity.

Keywords Klopman-Peradejordi-Gómez QSAR method, KPG method, QSAR, anticonvulsant activity, 2,5-disubstituted thiadiazoles, dendity functional theory, local atomic reactivity indices, electronic structure, epilepsy

Introduction

Epilepsy is a disorder that affects the brain and causes frequent bursts of electrical activity in the brain (seizures) that provisionally affect how it works [1, 2]. Magiorkinis et al., in a paper about the history of epilepsy stated that "the first description of an epileptic seizure appears in a text from 2000 BCE written in the Akkadian language, used in the region of Mesopotamia" [3]. Also the authors cited the Edwin Smith surgical papyrus (from Ancient Egypt, dated 1700 BCE), the Hamurabbi code (1790 BCE) and *The Sakikku* ("All Diseases", a Babylonian medical text dated 1067–1046 BCE), as sources mentioning epilepsy [3]. Later, epilepsy was considered in Ancient Greece as being "the sacred disease". Let us remember that the Persian King Cambyses II, the hero Hercules, the great Socrates, Julius Caesar (dictator in perpetuity and not Emperor as Magiorkinis et al. stated) and possibly Platon, Empedocles, Ajax and the Sibyls were epileptics (there is no consensus regarding some names) [3]. For later historical aspects we refer the reader to Magiorkinis et al. article [3].

Following Pedley [4], "seizures are discrete epileptic events, the manifestations of transient, hypersynchronous, abnormal neuronal behavior… The particular features of any single seizure depend upon whether most or only apart of the cerebral cortex is involved from the beginning, the functions of the cortical areas where the seizures

originates, the subsequent pattern of spread of abnormal electrical discharge within the brain, and the extent to which subcortical and brainstem areas are engaged. Thus, seizures reflect a temporary physiological dysfunction of the brain which evolves during the ictus and resolves postictally". Then, "epilepsy is a chronic disorder or, more accurately, group of chronic disorders, the indispensable feature of which is recurrent, unprovoked seizures. In a given patient with epilepsy, several different seizure types often coexist, and there may be variations in the pattern expressed by individual seizure types" [4].

In general, there is a surgical management and a non-surgical therapy for epilepsy. Epilepsy classification provides a framework for diagnosis [5]. As Wirrell states about the necessity of classification "epilepsy does not represent a single disorder, but rather is a collection of diverse conditions and syndromes which result in a lowered predisposition to unprovoked seizures. These disorders differ significantly in their response to specific therapies, their association with specific comorbidities, and their long- term seizure outcomes. Classification provides a scaffolding to help us organize these dive [5] disorders". The International League Against Epilepsy (ILAE) presented a Classification of the Epilepsies in 2017 [5, 6].

About twenty antiseizure medications (ASM) are now approved in the USA for use in the treatment of epilepsy. We can cite carbamazepine, clonazepam, phenobarbital, phenytoin, cannabidiol and zonisamide as examples. Kanth, Clark and Britton clearly state that "selecting a particular ASM for a given patient requires consideration of several factors. These include seizure type, medical comorbidities, side-effect profile, concurrent medical therapies, drug–drug interaction potential, gender, age, ease of use, clinical urgency, and cost" [7]. The necessity of new drugs for the treatment of epilepsy has led to the synthesis and testing of many families of molecules [8-28]. Usually, the anticonvulsant activity is determined by the maximal electroshock seizure (MES) in mice that identifies compounds which prevent seizure spread (also, the method of subcutaneous pentylenetetrazol-induced seizures in mice is used) [29, 30].

Recently a paper reporting MES results for a series of 2,5-disubstituted thiadiazoles was published [21]. The authors also report data suggesting an involvement of benzodiazepine receptors in the anticonvulsant action of these chemicals. With the aim of providing more information about the electronic determinants regulating the anticonvulsant activity, we present here the resuts of a quantum-chemical study searching for formal quantitative relationships (FQSAR) between the electronic structure and anticonvulsant activities of the abovementioned compounds.

Selection of biological data

The selected molecules are a group of 2,5-disubstituted thiadiazoles and were selected from a recent study [3]. Their general formula and biological activity are displayed, respectively, in Fig. 1 and Table 2. The anticonvulsant activity was determined by the maximal electroshock seizure method in mice.

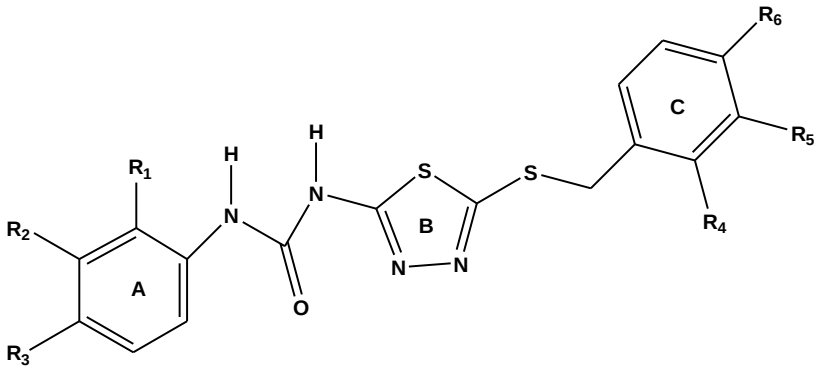

Figure 1: General formula of 2,5-disubstituted thiadiazoles

Table 1: 2,5-disubstituted thiadiazoles and anticonvulsant activity

Mol.	R_1	R_2	R_3	R_4	R_5	R_6	log (ED_{50}) (MES)
1	H	H	H	H	H	H	0.37
2	H	H	CH_3	H	H	H	0.53
3	H	H	F	H	H	H	0.50
4	H	H	Cl	H	H	H	0.55
5	Br	H	H	H	H	H	0.02
6	H	Cl	Cl	H	H	H	0.53
7	H	H	H	H	OCH_3	H	0.06
8	H	H	CH_3	H	OCH_3	H	0.56
9	Br	H	H	H	OCH_3	H	0.10
10	H	H	Cl	H	Cl	H	0.37
11	H	H	F	Cl	H	Cl	-0.19
12	H	H	H	H	NO_2	H	0.06
13	H	H	CH_3	H	NO_2	H	0.39
14	Br	H	H	H	NO_2	H	0.47

Figure 2 shows the histogram of frequencies for log (ED_{50}) and Fig. 3 displays the Box-Whiskers plot of log(ED_{50}) values with median and quartile values.

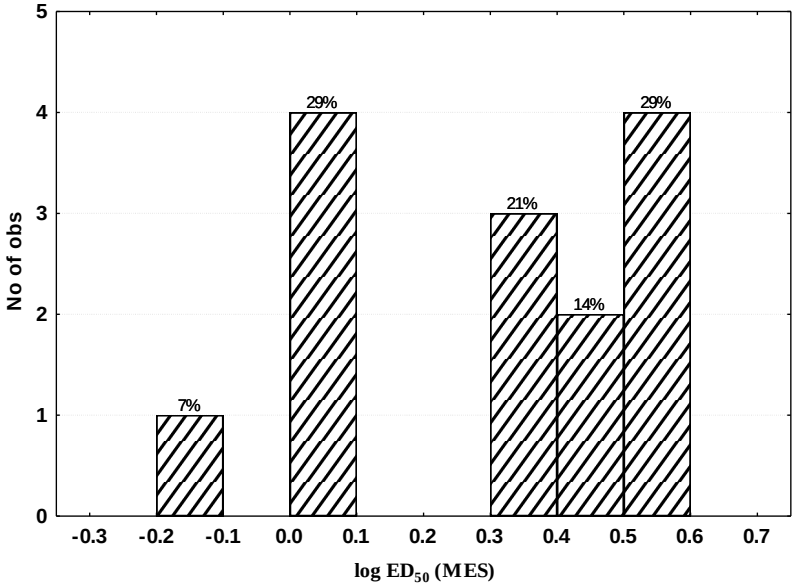

Figure 2: Histogram of frequencies for log(ED_{50})

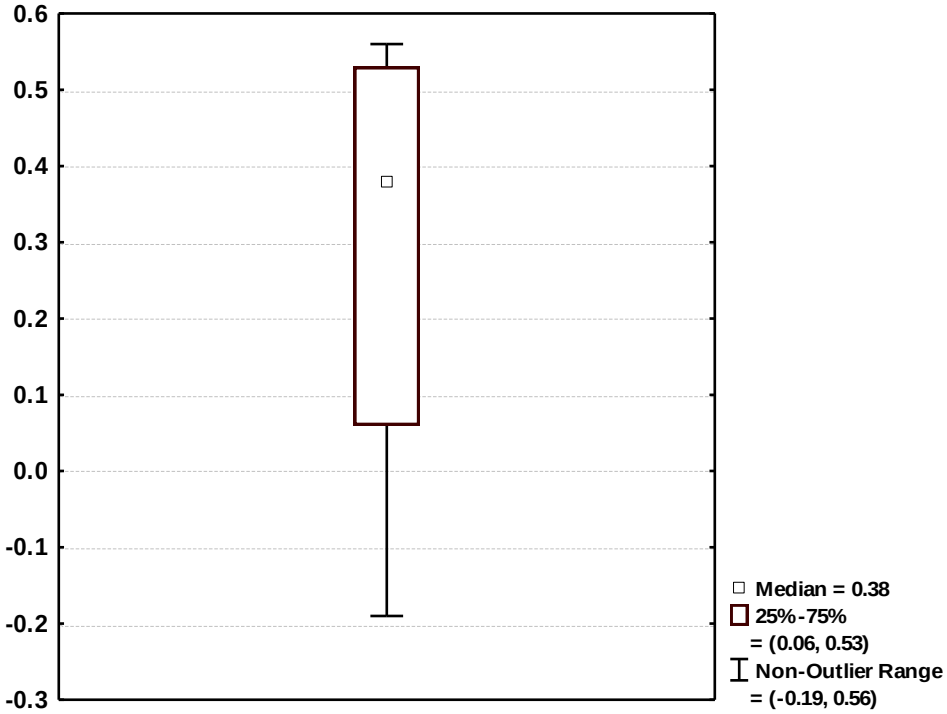

Figure 3: Box-Whiskers plot of log(ED_{50}) values

We can see that no outliers or extremes exist in the data set.

Models, methods and calculations

The model

The model to generate formal quantitative structure-activity relationships is based on the following master linear equation [31-42]:

$$\log(ED_{50}) = a + b\log(M_D) + \sum_{o=1}^{subs}\rho_o + \sum_{i=1}^{Z}\left[e_i Q_i + f_i S_i^E + s_i S_i^N\right] +$$
$$+\sum_{i=1}^{Z}\sum_{m=(HOMO-2)*,i}^{(HOMO)*,i}\left[h_i(m)F_i(m*) + j_i(m)S_i^E(m*)\right] +$$
$$+\sum_{i=1}^{Z}\sum_{m'=(LUMO)*,i}^{(LUMO+2)*,i}\left[r_i(m')F_i(m'*) + t_i(m')S_i^N(m'*)\right] +$$
$$+\sum_{i=1}^{Z}\left[g_i\mu_i^* + k_i\eta_i^* + o_i\omega_i^* + z_i\zeta_i^* + w_j Q_i^{*,max}\right] \quad (1)$$

with a, b, e_i, f_i, s_i $h_i(m)$, $j_i(m)$, $r_i(m')$, $t_i(m')$, g_i, k_i, o_i, z_i and w_i are constants to be determined, M_{D_i} is the mass of the drug, ρ_o is the orientational effect of the o-th substituent, Q_j is the net charge of the atom j, S_j^E and S_j^N are, respectively, the total atomic electrophilic and nucleophilic superdelocalizabilities of atom j, $F_j(m)$ and $F_j(m')$ are respectively the electron populations (Fukui index) of the occupied (m) and vacant (m′) local molecular orbitals (OMs) localized on atom j and $S_j^E(m)$ is the electrophilic superdelocalizability of the local OM m localized on

atom j. The last terms, derived by one of the authors [37], are: μ_j is the local atomic electronic chemical potential of atom j, η_j is the local atomic hardness of the atom j, ω_j is the local atomic electrophilicity of atom j, ς_j is the local atomic softness of the atom j, $Q_j^{\max}$ j is the maximum amount of electronic charge that atom j can accept (they are not the indices from Density Functional Theory, having the same units that the global equivalents). The MOs having an asterisk (*) correspond to the Local Molecular Orbitals (LMO) of each atom. For atom p, the LMOs correspond to the subset of the molecule's MOs having an electron population greater than 0.01e on p. In this study, we have considered the three highest occupied local MOs and the three lowest empty local MO of each atom. The index Z in the summations is defined below. Then, for a system of n molecules, we have n equations. The first condition that the system of equations 1 must met in order to be solved is that each equation must have the same number of terms. This condition is satisfied only by selecting and using only a group of atoms common to all the molecules. This group is called the common skeleton (see below) [41]. The number of atoms of this common skeleton defines the index Z of Eq. 1. The second condition is that we must have at least the same number of equations than the total number of indices of the common skeleton and the other terms of Eq. 1. For example if we have 20 atoms represented by 400 local atomic reactivity indices, we need at least 400 equations! Because of this reason, we used the linear multiple regression analysis (LMRA) to detect those indices associated with the variation of the values of the biological activity analyzed. The common skeleton used in this work is shown in figure 4. This method is called the Klopman-Peradejordi-Gómez (KPG) FQSAR method.

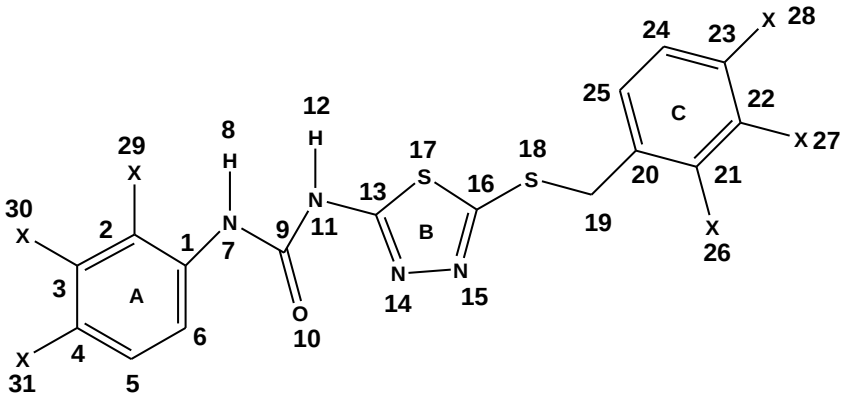

Figure 4: Common skeleton

This skeleton is composed by 31 atoms. The X's design the atoms of the substituents that are directly bonded to the skeleton. About 70 articles attest the success of this methodology applied to many different *in vitro* and *in vivo* molecular systems and several biological activities [43-53].

Calculations

The electronic structure of all molecules was calculated within the Density Functional Theory (DFT) at the B3LYP/6-31g(d,p) level after full geometry optimization. The Gaussian suite of programs was used [54]. All the information needed to compute the numerical values for the local atomic reactivity indices was obtained from the Gaussian results with the D-Cent-QSAR software [55]. All electron populations smaller than or equal to 0.01e are considered as being zero [37]. Negative electron populations appearing in Mulliken Population Analysis were corrected as usual [56]. Since the resolution of the system of linear equations is not possible because we have not enough molecules, we made use of Linear Multiple Regression Analysis (LMRA) techniques to find the best solution. For this case, a matrix containing the dependent variable ($\log(ED_{50})$ in this case) and the local atomic reactivity indices of all atoms of the common skeleton as independent variables was built The Statistica software was used for LMRA [57].

Results

The best equation obtained was:

$$\log(ED_{50})=0.37+0.18S_{28}^{N}(LUMO)^{*}+1.24F_{27}(HOMO\text{-}2)^{*}-0.96F_{24}(LUMO+2)^{*}+$$
$$+0.02S_{4}^{N}(LUMO+2)^{*} \quad (2)$$

with n=14, adj-R^2=0.93, F(4,9)=42.445 (p<0.00001) and SD=0.06. No outliers were detected and no residuals fall outside the ±2σ limits. Here, $S_{28}^{N}(LUMO)^{*}$ is the nucleophilic superdelocalizability of the lowest empty local molecular orbital (MO) of atom 28, $F_{27}(HOMO\text{-}2)^{*}$ is the electron population of the third highest occupied local MO of atom 27, $F_{24}(LUMO+2)^{*}$ is the electron population on the third lowest empty local MO of atom 24 and $S_{4}^{N}(LUMO+2)^{*}$ is the nucleophilic superdelocalizability of the third lowest empty MO of atom 4.

Tables 2 and 3 show the beta coefficients, the results of the t-test for significance of coefficients and the matrix of squared correlation coefficients for the variables of Eq. 2. There are no significant internal correlations between independent variables (Table 3). Figure 5 displays the plot of observed *vs.* calculated values of $\log(ED_{50})$.

Table 2: Beta coefficients and t-test for significance of coefficients in Eq. 2

Variable	Beta	t(9)	p-value
$S_{28}^{N}(LUMO)^{*}$	0.80	8.97	0.000009
$F_{27}(HOMO\text{-}2)^{*}$	0.67	8.15	0.00002
$F_{24}(LUMO+2)^{*}$	-0.47	-5.83	0.0003
$S_{4}^{N}(LUMO+2)^{*}$	0.35	3.70	0.005

Table 3: Matrix of squared correlation coefficients for the variables in Eq. 2

	$S_{28}^{N}(LUMO)^{*}$	$F_{27}(HOMO\text{-}2)^{*}$	$F_{24}(LUMO+2)^{*}$	$S_{4}^{N}(LUMO+2)^{*}$
$S_{28}^{N}(LUMO)^{*}$	1			
$F_{27}(HOMO\text{-}2)^{*}$	0.05	1		
$F_{24}(LUMO+2)^{*}$	0.11	0.00	1	
$S_{4}^{N}(LUMO+2)^{*}$	0.25	0.15	0.10	1

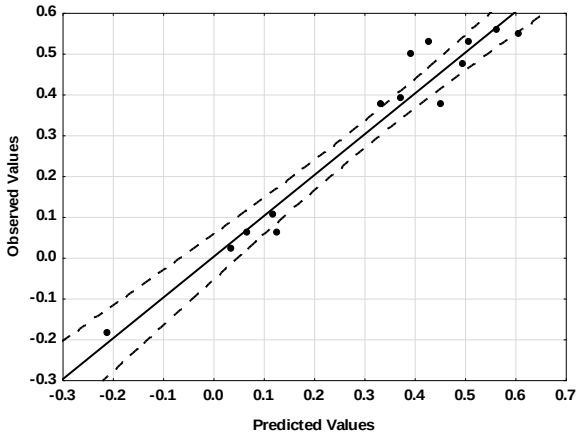

Figure 5: Plot of predicted vs. observed log(ED_{50}) values (Eq. 2). Dashed lines denote the 95% confidence interval.

The associated statistical parameters of Eq. 2 indicate that this equation is statistically significant and that the variation of the numerical values of a group of four local atomic reactivity indices of atoms constituting the common skeleton explains about 93% of the variation of $\log(ED_{50})$. Figures 6, 7 and 8 show, respectively, the plot of predicted values vs. residuals scores, the plot of residual *vs.* deleted residuals and the normal probability plot of residuals.

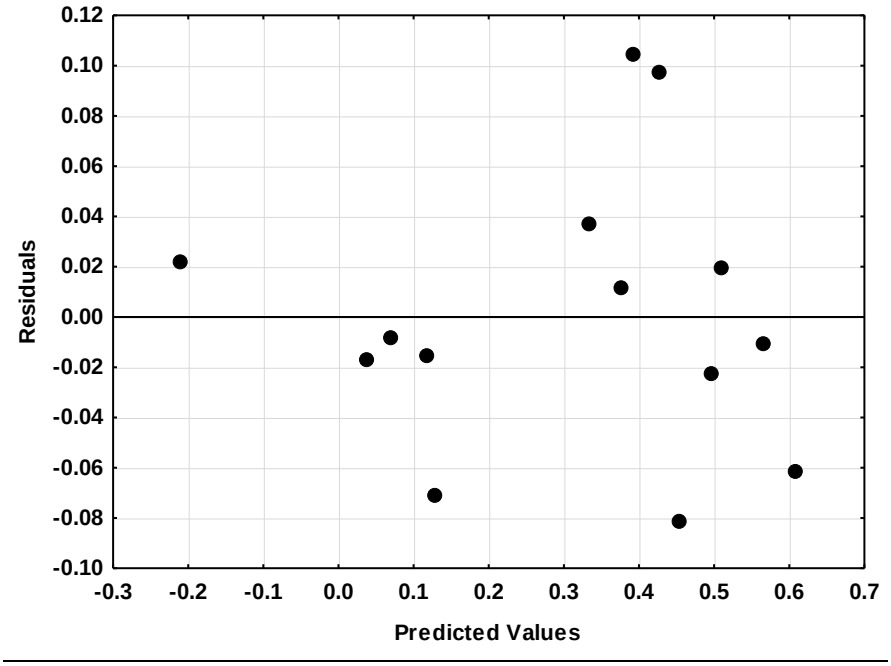

Figure 6: Plot of predicted values vs. residuals scores

Because the points do not show any kind of ordering or tendency, this plot supports the idea that the linear equation 1 is an acceptable first approach to study the anticonvulsant activity of these molecules.

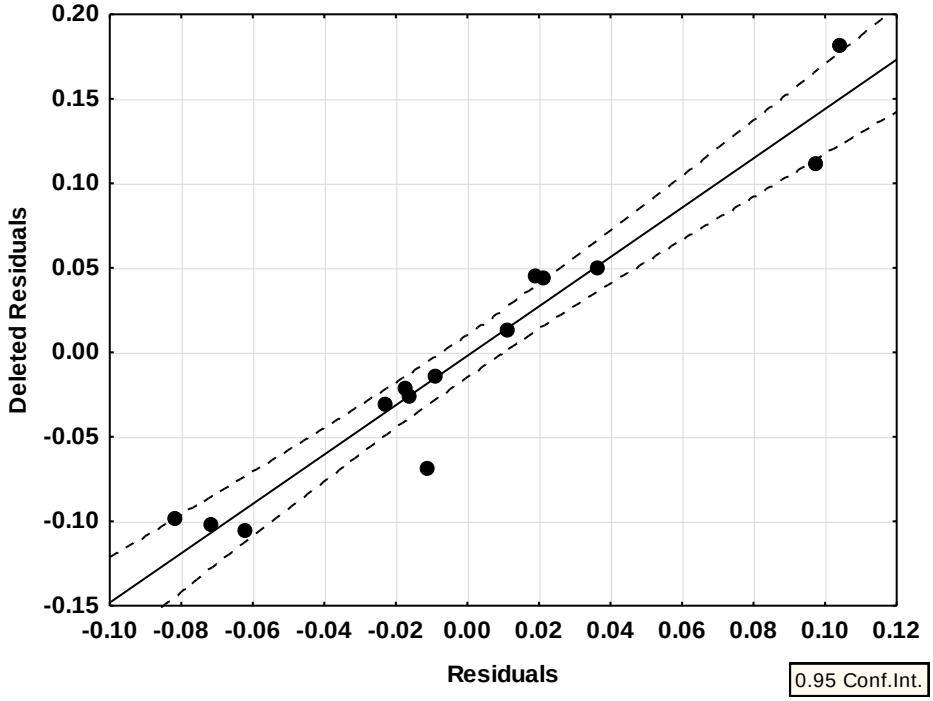

Figure 7: Plot of residual vs. deleted residuals

In a very good equation, all points are inside the 95% confidence interval. In this case, we have one point outside the confidence interval, strongly suggesting that this molecule probably has additional interactions involving atoms that do not belong to the common skeleton. So far, we have not been able to design a method to identify these possible extra interactions.

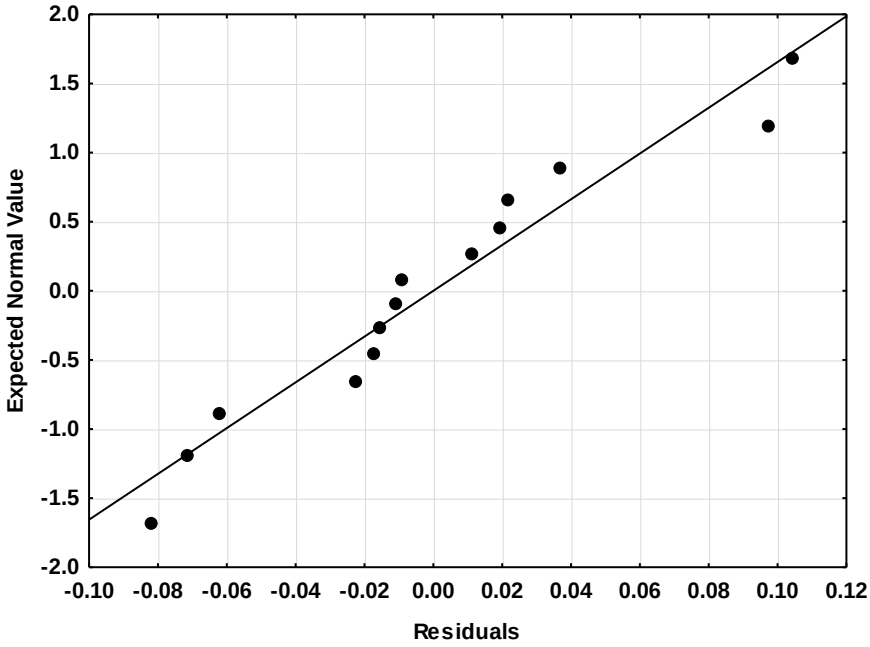

Figure 8: Normal probability plot of residuals

In Fig. 8, there is a lack of fitting and the data does not form a pattern around the straight line. Therefore, our use of a linear model is appropriate. Then, figures 6, 7 and 8 provide support to state that the linear equation 1 is a good first approximation to analyze the anticonvulsants activity.

Local Molecular Orbitals

If a local atomic reactivity index of an inner occupied local MO (i.e., (HOMO-1)* and/or (HOMO-2)*) or of a higher empty MO ((LUMO+1)* and/or (LUMO+2)*) appears in the equation, this means that the remaining of the upper occupied local MOs (if (HOMO-2)* appears, upper means (HOMO-1)* and (HOMO)*) or the remaining of the empty MOs (if (LUMO+1)* appears, lower means the (LUMO)*) also contribute to the interaction. Their absence in the equation only means that the variation of their numerical values does not account for the variation of the numerical value of the biological property.

Table 4: The local MO structure of atoms 4, 24, 27 and 28 of equation 2 (see Fig. 4). Nomenclature: Molecule (HOMO) / (HOMO-2)* (HOMO-1)* (HOMO)* - (LUMO)* (LUMO+1)* (LUMO+2)*.

Mol.	Atom 4	Atom 24	Atom 27	Atom 28
1 (89)	86π88π89π- 90π91π 92π	87π88π89π- 91π93π94π	69σ76σ77σ- 98σ99σ100σ	75σ76σ78σ- 98σ99σ100σ
2 (93)	85π87σ93π- 94π95π97π	89π90π92π- 95π96π97π	70σ79σ80σ- 102σ103σ105σ	77σ79σ82σ- 102σ103σ105σ
3 (93)	89π91π92π- 94π95π96π	90π91π92π- 94π96π98π	80σ81σ82σ- 104σ105σ107σ	80σ81σ82σ- 104σ105σ108σ
4 (97)	93π96π97π- 98π99π100π	94π95π96π- 99π102π103π	83σ84σ85σ- 108σ110σ111σ	82σ83σ84σ- 108σ110σ111σ
5 (106)	104π105π106π- 107π108π109π	104π105π106π- 109π110π112π	91σ92σ93σ- 117σ118σ119σ	91σ92σ93σ- 117σ118σ119σ
6 (105)	102π104π105π- 106π107π108π	103π104π105π- 109π110π112π	82σ90σ91σ- 116σ117σ118σ	89σ90σ93σ- 116σ117σ118σ
7 (97)	92π95π96π-	94π95π97π-	87π95π97π-	81σ82σ85σ-

	98π99π100π	99π101π102π	102π108π109π	107σ108σ109σ
8 (101)	98π99π100π- 103π104π105π	99π100π101π- 103π105π106π	90π99π101π- 106π126σ127σ	83σ86σ89σ- 110σ112σ113σ
9 (114)	111π112π113π- 115π116π117π	112π113π114π- 116π118π120π	104π113π114π- 120π122π138σ	96σ98σ100σ- 124σ125σ127σ
10 (105)	101π104π105π- 106π107π108π	100π102π103π- 107π109π110π	96π102π103π- 110π112π113π	87σ88σ89σ- 112σ113σ114σ
11 (109)	100π105π109π- 111π114π115π	106π107π108π- 110π111π112π	89σ90σ91σ- 116σ122σ124σ	106π107π108π- 111π116π117π
12 (100)	90π94σ100π- 102π103π105π	95π96π99π- 101π102π103π	88π89σ92π- 101π107π110π	81σ82σ84σ- 110σ111σ112σ
13 (104)	97σ98π104π- 106π107π108π	99π100π103π- 105106π107π	92σ95π96π- 105π110π111π	85σ86σ88σ- 115σ117σ118σ
14 (117)	114π116π117π- 119π120π121π	111π112π113π- 118π119π120π	105σ106σ108π- 118π124π126π	96σ98σ99σ- 129σ131σ133σ

Discussion

First, it is necessary to mention a very important point. The activity analyzed here was measured *in vivo*. In this case, drug molecules may go through multiple steps (for example, at the n-th step, molecules must cross a pore), some steps may have a complex mechanism (for example, to cross a pore, molecules must consecutively interact with j unknown sites). Therefore, it seems logical to state that a necessary condition to obtain good *in vivo* structure-activity relationships is that all the stages and all the mechanisms within each stage must be the same for the entire group of molecules under study. This will allow the KPG method to yield good results. Note that this condition can be also applied to some *in vitro* studies such as anti-proliferative activities, carcinogenicity, etc. As the exact process explaining the *in vivo* anticonvulsant activity is not known, we are not able to assign the terms appearing in Eq. 1 to a specific step. However, this is not an obstacle to analyze the resulting equation.

Table 2 shows that the importance of variables in Eq. 1 is S_{28}^{N}(LUMO)*> F_{27}(HOMO-2)* >> F_{24}(LUMO+2)*> S_{4}^{N}(LUMO+2)*. A high anticonvulsant activity is then associated with low numerical values for S_{28}^{N}(LUMO)*, low numerical values for F_{27}(HOMO-2)*, high numerical values for F_{24}(LUMO+2)* and low numerical values for S_{4}^{N}(LUMO+2)*.

Atom 28 is the first atom of the substituent bonded to atom 23 (Fig. 4). Table 1 shows that it can be hydrogen or chlorine. It is important to mention that atom 23 does not appear in Eq. 1. Small numerical values for S_{28}^{N}(LUMO)* are associated with high anticonvulsant activity. This means that to obtain these small numerical values we must

increase the $(LUMO)_{28}^{*}$ energy, making this atom a bad electron acceptor. We need to find an explanation for C23-H28….X and C23-Cl28….X interactions. For hydrogen, a possibility is the formation of a C23-H28…X (with X= O, N, S) weak hydrogen bond. Note that in the case of H substituents the local $(HOMO)_{28}^{*}$ and the local $(LUMO)_{28}^{*}$ do not coincide with the molecular HOMO and LUMO and that all local MOs have a σ nature (Table 4). In the case of the chlorine substituent, the local $(HOMO)_{28}^{*}$ and the local $(LUMO)_{28}^{*}$ are energetically close to the molecule's HOMO and LUMO and both have a π nature (Table 4). A possibility is that chlorine participates in a C23-Cl28…X interaction through its $(HOMO)_{28}^{*}$ (an halogen interaction).

Atom 27 is the first atom of the substituent bonded to atom 22 (Fig. 4). Table 1 shows that it can be hydrogen, chlorine, nitro or methoxy. Small numerical values for F_{27}(HOMO-2)* are associated with high anticonvulsant activity. Our working hypothesis states that in this case F_{27}(HOMO-1)* and F_{27}(HOMO)* must also have small numerical values. Then atom 27 should be a bad electron donor. For hydrogen substituents the local $(HOMO)_{27}$* and $(LUMO)_{27}$* have a σ nature and their energies are very far from the molecular HOMO and LUMO energies like in the previous case (Table 4). For the case of the hydrogen substituent, we may suggest that H27 is involved in a weak C22-H27…X (with X=O, N, S) hydrogen bond (see the case of atom 28 above). For the case of the oxygen atom of the methoxy substituents, the local $(HOMO)_{27}^{*}$ coincides with the molecular HOMO and has a π nature in all cases (Table 4). The chlorine substituent has a π $(HOMO)_{27}^{*}$ that is energetically close to the molecular HOMO (Table 4). Also, in chlorine the $(LUMO)_{27}^{*}$ has a π nature but it is energetically far from the molecule's LUMO (Table 4). For these cases, we suggest a second site for π-π interactions. The local frontier MOs of all the N atoms of the nitro substituents have a π nature (Table 4) and the local $(HOMO)_{27}$* is energetically far from the molecular HOMO. The local $(LUMO)_{27}^{*}$ coincides with the molecular LUMO. For this case, we may suggest that there is a C22-N27…X interaction with X being an electron-rich center.

Atom 24 is a carbon in ring C (Fig. 4). High numerical values for F_{24}(LUMO+2)* are associated with high anticonvulsant activity. Our working hypothesis states that in this case F_{24}(LUMO+1)* and F_{24}(LUMO)* should have high numerical values. Table 4 shows that the three highest occupied local MOs and the three lowest empty local MOs have a π nature. The local frontier MOs are energetically close or coincide with the molecular HOMO and LUMO. This suggests that atom 24 should be interacting with an electron-rich center (an aromatic system, an anion, etc.).

Atom 4 is a carbon in ring A (Fig. 4). Small numerical values for S_4^N(LUMO+2)* are associated with high anticonvulsant activity. Our working hypothesis states that in this case S_4^N(LUMO+1)* and S_4^N(LUMO)* should have also small numerical values. This means that atom 4 will not interact with electron-rich centers but with electron-deficient ones. Therefore, a fluorine atom or any other substituent extracting electron from atom 4 is suitable. All the suggestions are displayed in the partial 2D pharmacophore of Fig. 9.

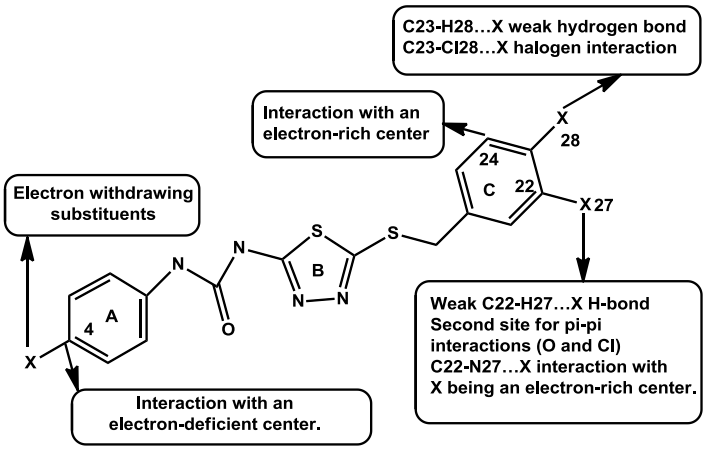

Figure 9: Partial 2D pharmacophore for in vivo anticonvulsant activity

Conclusion

In summary, for a group of 2,5-disubstituted thiadiazoles we found a statistically significant equation relating *in vivo* anticonvulsant activity to some local atomic reactivity indices belonging to a common skeleton. This equation allowed us to suggest possible interactions that should help to design and test more active molecules.

Conflicts of Interest

The authors declare that they have no competing interests.

References

[1]. Cascino, G. D.; Sirven, J. I.; Tatum, W. O. *Epilepsy*. John Wiley & Sons, Ltd: Chichester, UK, 2021.
[2]. Resor, S. R.; Henn, K. *The medical treatment of epilepsy*. CRC Press: Boca Raton, USA, 2020.
[3]. Magiorkinis, E.; Sidiropoulou, K.; Diamantis, A. Hallmarks in the history of epilepsy: epilepsy in antiquity. *Epilepsy & behavior* 2010, 17, 103-108.
[4]. Pedley, T. A. Classification of seizures and epilepsy. In *The medical treatment of epilepsy*, Resor, S. R.; Henn, K., Eds. CRC Press: Boca Raton, USA, 2020; pp 3-14.
[5]. Wirrell, E. C. Classification of Seizures and the Epilepsies. In *Epilepsy*, Cascino, G. D.; Sirven, J. I.; Tatum, W. O., Eds. John Wiley & Sons, Ltd: Chichester, UK, 2021; pp 11-22.
[6]. Scheffer, I. E.; Berkovic, S.; Capovilla, G.; Connolly, M. B.; French, J.; Guilhoto, L.; Hirsch, E.; Jain, S.; Mathern, G. W.; Moshé, S. L. ILAE classification of the epilepsies: position paper of the ILAE Commission for Classification and Terminology. *Epilepsia* 2017, 58, 512-521.
[7]. Kanth, K. M.; Clark, S.; Britton, J. W. Antiseizure Medication Therapy. In *Epilepsy*, Cascino, G. D.; Sirven, J. I.; Tatum, W. O., Eds. John Wiley & Sons, Ltd: Chichester, UK, 2021; pp 179-215.
[8]. Zhang, S.-S.; Liu, W.-H.; He, Z.-W.; Tan, Q.-W.; Guan, L.-P. Synthesis of Chromen-1-phenylpropan-1-one Derivatives and their Antidepressant/Anticonvulsant Activities. *Letters in Drug Design & Discovery* 2021, 18, 1136-1145.
[9]. Tan, Q.-W.; He, L.-Y.; He, Z.-W.; Liu, W.-H.; Zhang, S.-S.; Lin, L.; Yang, H.-L.; Guan, L.-P. Design, synthesis, and antidepressant/anticonvulsant activities of 3H-benzo [f] chromen chalcone derivatives. *Medicinal Chemistry Research* 2021, 1-11.
[10]. Song, M.X.; Huang, Y.S.; Zhou, Q.G.; Deng, X.Q.; Yao, X.D. Synthesis of ring-opened derivatives of triazole-containing quinolinones and their antidepressant and anticonvulsant activities. *Bioorganic Chemistry* 2021, 106, 104505.
[11]. Patel, S. The Antiepileptic Effect of Synthesized Derivatives of Quinazoline-4 (3H)-One. *BR Nahata Smriti Sansthan International Journal of Phramaceutical Sciences & Clinical Research* 2021, 1.
[12]. Obniska, J.; Góra, M.; Rapacz, A.; Sałat, K.; Rybka, S.; Abram, M.; Jakubiec, M.; Kamiński, K. Synthesis, anticonvulsant, and antinociceptive activity of new 3-(3-methyl-2, 5-dioxo-3-phenylpyrrolidin-1-yl) propanamides and 3-phenyl-butanamides. *Archiv der Pharmazie* 2021, 354, 2000225.
[13]. Nath, R.; Yar, M. S.; Pathania, S.; Grover, G.; Debnath, B.; Akhtar, M. J. Synthesis and anticonvulsant evaluation of indoline derivatives of functionalized aryloxadiazole amine and benzothiazole acetamide. *Journal of Molecular Structure* 2021, 1228, 129742.
[14]. Mishra, C. B.; Kumari, S.; Angeli, A.; Bua, S.; Mongre, R. K.; Tiwari, M.; Supuran, C. T. Discovery of potent carbonic anhydrase inhibitors as effective anticonvulsant agents: drug design, synthesis, and in vitro and in vivo investigations. *Journal of Medicinal Chemistry* 2021, 64, 3100-3114.
[15]. Lingappa, M.; Guruswamy, V.; Bantal, V. Synthesis and characterization of 4-amino-4H-1, 2, 4-triazole derivatives: Anticonvulsant activity. *Current Chemistry Letters* 2021, 10, 33-42.
[16]. Kerzare, D. R.; Menghani, S. S.; Rarokar, N. R.; Khedekar, P. B. Development of novel indole-linked pyrazoles as anticonvulsant agents: A molecular hybridization approach. *Archiv der Pharmazie* 2021, 354, 2000100.

[17]. Góra, M.; Czopek, A.; Rapacz, A.; Gębska, A.; Wójcik-Pszczoła, K.; Pękala, E.; Kamiński, K. Synthesis, Anticonvulsant, and Antinociceptive Activity of New 3-(2-Chlorophenyl)-and 3-(3-Chlorophenyl)-2, 5-dioxo-pyrrolidin-1-yl-acetamides. *Molecules* 2021, 26, 1564.

[18]. Drabik, M.; Głuszak, M.; Wróblewska-Łuczka, P.; Plewa, Z.; Jankiewicz, M.; Kozińska, J.; Florek-Łuszczki, M.; Plech, T.; Łuszczki, J. J. Anticonvulsant Effectiveness and Neurotoxicity Profile of 4-butyl-5-[(4-chloro-2-methylphenoxy) methyl]-2, 4-dihydro-3 H-1, 2, 4-triazole-3-thione (TPL-16) in Mice. *Neurochemical Research* 2021, 46, 396-410.

[19]. Abram, M.; Rapacz, A.; Latacz, G.; Szulczyk, B.; Kalinowska-Tłuścik, J.; Otto-Ślusarczyk, D.; Struga, M.; Kamiński, R. M.; Kamiński, K. Asymmetric synthesis and in vivo/in vitro characterization of new hybrid anticonvulsants derived from (2, 5-dioxopyrrolidin-1-yl) phenylacetamides. *Bioorganic Chemistry* 2021, 109, 104751.

[20]. Abram, M.; Jakubiec, M.; Rapacz, A.; Mogilski, S.; Latacz, G.; Szulczyk, B.; Szafarz, M.; Socała, K.; Nieoczym, D.; Wyska, E. Identification of New Compounds with Anticonvulsant and Antinociceptive Properties in a Group of 3-substituted (2, 5-dioxo-pyrrolidin-1-yl)(phenyl)-Acetamides. *International journal of molecular sciences* 2021, 22, 13092.

[21]. Toolabi, M.; Khoramjouy, M.; Aghcheli, A.; Ayati, A.; Moghimi, S.; Firoozpour, L.; Shahhosseini, S.; Shojaei, R.; Asadipour, A.; Divsalar, K.; Faizi, M.; Foroumadi, A. Synthesis and radioligand-binding assay of 2,5-disubstituted thiadiazoles and evaluation of their anticonvulsant activities. *Archiv der Pharmazie* 2020, 353, 2000066.

[22]. Song, M.-X.; Huang, Y.; Wang, S.; Wang, Z.-T.; Deng, X.-Q. Design, synthesis, and evaluation of anticonvulsant activities of benzoxazole derivatives containing the 1,2,4-triazolone moiety. *Archiv der Pharmazie* 2019, 352, 1800313.

[23]. Zhang, H.-J.; Jin, P.; Wang, S.-B.; Li, F.-N.; Guan, L.-P.; Quan, Z.-S. Synthesis and Anticonvulsant Activity Evaluation of 4-Phenyl-[1,2,4]triazolo[4,3-a]quinazolin-5(4H)-one and Its Derivatives. *Archiv der Pharmazie* 2015, 348, 564-574.

[24]. Madaiah, M.; Prashanth, M. K.; Revanasiddappa, H. D.; Veeresh, B. Synthesis and Evaluation of 3-[(2,4-Dioxo-1,3,8-triazaspiro[4.6]undec-3-yl)methyl]benzonitrile Derivatives as Potential Anticonvulsants. *Archiv der Pharmazie* 2013, 346, 200-209.

[25]. Zhu, Q.; Pan, Y.; Xu, Z.; Li, R.; Qiu, G.; Xu, W.; Ke, X.; Wu, L.; Hu, X. Synthesis and potential anticonvulsant activity of new N-3-substituted 5, 5-cyclopropanespirohydantoins. *European journal of medicinal chemistry* 2009, 44, 296-302.

[26]. Özdemir, Z.; Kandilci, H. B.; Gümüşel, B.; Çalış, Ü.; Bilgin, A. A. Synthesis and studies on antidepressant and anticonvulsant activities of some 3-(2-furyl)-pyrazoline derivatives. *European journal of medicinal chemistry* 2007, 42, 373-379.

[27]. Marona, H. Synthesis and anticonvulsant effects of some aminoalkanolic derivatives of xanthone. *Die Pharmazie* 1998, 53, 672-676.

[28]. Kornet, M. J. Synthesis and anticonvulsant evaluation of N-aminosuccinimides. *Journal of pharmaceutical sciences* 1984, 73, 405-406.

[29]. Castel-Branco, M.; Alves, G.; Figueiredo, I.; Falcão, A.; Caramona, M. The maximal electroshock seizure (MES) model in the preclinical assessment of potential new antiepileptic drugs. *Methods Find Exp Clin Pharmacol*. 2009, 31, 101-106.

[30]. Mandhane, S. N.; Aavula, K.; Rajamannar, T. Timed pentylenetetrazol infusion test: a comparative analysis with sc PTZ and MES models of anticonvulsant screening in mice. *Seizure* 2007, 16, 636-644.

[31]. Peradejordi, F.; Martin, A. N.; Cammarata, A. Quantum chemical approach to structure-activity relationships of tetracycline antibiotics. *Journal of Pharmaceutical Sciences* 1971, 60, 576-582.

[32]. Gómez-Jeria, J. S. On some problems in quantum pharmacology I. The partition functions. *International Journal of Quantum Chemistry* 1983, 23, 1969-1972.

[33]. Gómez-Jeria, J. S. Modeling the Drug-Receptor Interaction in Quantum Pharmacology. In *Molecules in Physics, Chemistry, and Biology*, Maruani, J., Ed. Springer Netherlands: 1989; Vol. 4, pp 215-231.

[34]. Gómez-Jeria, J. S.; Ojeda-Vergara, M. Parametrization of the orientational effects in the drug-receptor interaction. *Journal of the Chilean Chemical Society* 2003, 48, 119-124.

[35]. Barahona-Urbina, C.; Nuñez-Gonzalez, S.; Gómez-Jeria, J. S. Model-based quantum-chemical study of the uptake of some polychlorinated pollutant compounds by Zucchini subspecies. *Journal of the Chilean Chemical Society* 2012, 57, 1497-1503.

[36]. Gómez-Jeria, J. S. *Elements of Molecular Electronic Pharmacology (in Spanish)*. 1st ed.; Ediciones Sokar: Santiago de Chile, 2013; p 104.

[37]. Gómez-Jeria, J. S. A New Set of Local Reactivity Indices within the Hartree-Fock-Roothaan and Density Functional Theory Frameworks. *Canadian Chemical Transactions* 2013, 1, 25-55.

[38]. Gómez-Jeria, J. S. Tables of proposed values for the Orientational Parameter of the Substituent. I. Monoatomic, Diatomic, Triatomic, n-CnH2n+1, O-n-CnH2n+1, NRR', and Cycloalkanes (with a single ring) substituents. *Research Journal of Pharmaceutical, Biological and Chemical Sciences* 2016, 7, 288-294.

[39]. Gómez-Jeria, J. S. Tables of proposed values for the Orientational Parameter of the Substituent. II. *Research Journal of Pharmaceutical, Biological and Chemical Sciences* 2016, 7, 2258-2260.

[40]. Gómez-Jeria, J. S.; Kpotin, G. Some Remarks on The Interpretation of The Local Atomic Reactivity Indices Within the Klopman-Peradejordi-Gómez (KPG) Method. I. Theoretical Analysis. *Research Journal of Pharmaceutical, Biological and Chemical Sciences* 2018, 9, 550-561.

[41]. Gómez-Jeria, J. S.; Robles-Navarro, A.; Kpotin, G.; Garrido-Sáez, N.; Gatica-Díaz, N. Some remarks about the relationships between the common skeleton concept within the Klopman-Peradejordi-Gómez QSAR method and the weak molecule-site interactions. *Chemistry Research Journal* 2020, 5, 32-52.

[42]. The results presented here are obtained from what is now a routinary procedure. For this reason, all papers have a similar general structure. This model contains *standard* phrases for the presentation of the methods, calculations and results because they do not need to be rewritten repeatedly and because the number of possible variations to use is finite. See: Hall, S., Moskovitz, C., and Pemberton, M. 2021. Understanding Text Recycling: A Guide for Researchers. Text Recycling Research Project. Online at textrecycling.org. In.

[43]. Gómez-Jeria, J. S.; Silva-Monroy, S. A quantum-chemical analysis of the relationships between electronic structure and inhibition of SARS-CoV-2 virus by a group of cyclic sulfonamide derivatives. *Chemistry Research Journal* 2021, 6, 54-70.

[44]. Gómez-Jeria, J. S.; Robles-Navarro, A.; Soza-Cornejo, C. A note on the relationships between electronic structure and serotonin 5-HT_{1A} receptor binding affinity in a series of 4-butyl-arylpiperazine-3-(1*H*-indol-3-yl)pyrrolidine-2,5-dione derivatives. *Chemistry Research Journal* 2021, 6, 76-88.

[45]. Gómez-Jeria, J. S.; Robles-Navarro, A.; Soto-Martínez, V. Quantum Chemical Analysis of the relationships between electronic structure and dopamine D_1 and D_5 receptor binding affinities in a series of 1-phenylbenzazepines. *Chemistry Research Journal* 2021, 6, 128-144.

[46]. Gómez-Jeria, J. S.; Ibertti-Arancibia, A. A DFT study of the relationships between electronic structure and dopamine D_1 and D_2 receptor affinity of a group of (S)-enantiomers of 11-(1,6-dimethyl-1,2,3,6-tetrahydropyridin-4-yl)-5*H*-dibenzo[b,e][1,4]diazepines. *Chemistry Research Journal* 2021, 6, 116-131.

[47]. Gómez-Jeria, J. S.; Crisóstomo-Cáceres, S. R.; Robles-Navarro, A. On the compatibility between formal QSAR results and docking results: the relationship between electronic structure and H5N1 (A/goose/Guangdong/SH7/2013) neuraminidase inhibition by some Tamiflu derivatives as an example. *Chemistry Research Journal* 2021, 6, 46-59.

[48]. Gómez-Jeria, J. S.; Valenzuela-Hueichaqueo, N. J. The relationships between electronic structure and human A_1 adenosine receptor binding affinity in a series of triazolopyridine derivatives. *Chemistry Research Journal* 2020, 5, 226-236.

[49]. Kpotin, G. A.; Bédé, A. L.; Houngue-Kpota, A.; Anatovi, W.; Kuevi, U. A.; Atohoun, G. S.; Mensah, J.-B.; Gómez-Jeria, J. S.; Badawi, M. Relationship between electronic structures and antiplasmodial activities of xanthone derivatives: a 2D-QSAR approach. *Structural Chemistry* 2019, 30, 2301-2310.

[50]. Gómez-Jeria, J. S.; Soto-Morales, F.; Rivas, J.; Sotomayor, A. A theoretical structure-affinity relationship study of some cannabinoid derivatives. *Journal of the Chilean Chemical Society* 2008, 53, 1393-1399.

[51]. Gómez-Jeria, J. S.; Lagos-Arancibia, L.; Sobarzo-Sánchez, E. Theoretical study of the opioid receptor selectivity of some 7-arylidenenaltrexones. *Boletin de la Sociedad Chilena de Quimica* 2003, 48, 61-66.

[52]. Gómez-Jeria, J. S.; Morales-Lagos, D.; Cassels, B. K.; Saavedra-Aguilar, J. C. Electronic structure and serotonin receptor binding affinity of 7-substituted tryptamines. *Quantitative Structure-Activity Relationships* 1986, 5, 153-157.

[53]. Gómez-Jeria, J. S.; Morales-Lagos, D.; Rodriguez-Gatica, J. I.; Saavedra-Aguilar, J. C. Quantum-chemical study of the relation between electronic structure and pA2 in a series of 5-substituted tryptamines. *International Journal of Quantum Chemistry* 1985, 28, 421-428.

[54]. Frisch, M. J.; Trucks, G. W.; Schlegel, H. B.; Scuseria, G. E.; Robb, M. A.; Cheeseman, J. R.; Scalmani, G.; Barone, V.; Petersson, G. A.; Nakatsuji, H.; Li, X.; Caricato, M.; Marenich, A. V.; Bloino, J.; Janesko, B. G.; Gomperts, R.; Mennucci, B.; Hratchian, H. P. *Gaussian 16 16Rev. A.03*, Gaussian: Pittsburgh, PA, USA, 2016.

[55]. Gómez-Jeria, J. S. *D-Cent-QSAR: A program to generate Local Atomic Reactivity Indices from Gaussian16 log files*, v. 1.0; Santiago, Chile, 2020.

[56]. Gómez-Jeria, J. S. An empirical way to correct some drawbacks of Mulliken Population Analysis (Erratum in: J. Chil. Chem. Soc., 55, 4, IX, 2010). *Journal of the Chilean Chemical Society* 2009, 54, 482-485.

[57]. Statsoft. *Statistica v. 8.0*, 2300 East 14 th St. Tulsa, OK 74104, USA, 1984-2007.